Available online at www.sciencedirect.com

SciVerse ScienceDirect

Physics Procedia 32 (2012) 88 – 94

Physics Procedia

18th International Vacuum Congress (IVC-18)

Activation of photoluminescence of multilayer arrays of silicon rich oxide by oxidation at different temperatures

E. Quiroga-González[a*], W. Bensch[b], M. Aceves-Mijares[c], Z. Yu[d]

[a] *Institute for Material Science of the University of Kiel. Germany*
[b] *Institute for Inorganic Chemistry of the University of Kiel. Germany.*
[c] *National Institute for Astrophysics, Optics and Electronics. Mexico.*
[d] *Tianjin Lishen Battery Joint-Stock Co. Ltd. China.*

*E-mail: equiroga@ieee.org

Abstract

Multilayer structures composed of layers of silicon rich oxide (SRO) with high and low Si content have been prepared by low pressure chemical vapor deposition. These multilayers were oxidized at 800, 900, 1000, and 1100 °C under dry oxygen to study the possibility of photoluminescence production. Only the samples oxidized at 1000 and 1100 °C present this effect. The spectra of the two photoluminescent samples can be deconvoluted in two asymmetric peaks positioned at 1.53 and 1.73 eV. The peak at 1.73 eV has been previously found in Silicon Rich Oxide with low Si content and without Si-nanocrystals, and has been ascribed to defects in the silicon oxide matrix. The other peak has been attributed to defects in the Si-nanocrystals/SiO_2 interface.

PACS: 68.55.ag; 78.55.-m; 78.67.Pt

Kyewords: Silicon rich oxide; Si nanocrystals; photoluminescence; defects; multilayer

1. Introduction

Silicon rich oxide (SRO), also known as silicon rich silicon oxide or off-stoichiometric silicon oxide, is a multiphase material composed of silicon oxides and Si agglomerates [1, 2]. Silicon nanocrystals (Si-nCs) grow by segregation of the Si excess from the silicon oxides during thermal treatments at high temperatures [3]. An indicator of the Si content in this material is the parameter Ro, which is the ratio of the partial pressure of the precursor gases (for example N_2O/SiH_4) when it is prepared by gas phase deposition methods like CVD (chemical vapor deposition). When the Si-nCs are smaller than 5 nm in diameter (the Bohr radius for electrons in crystalline Si [4]) they may behave as quantum dots exhibiting quantum confinement effects in three dimensions. Si-quantum dots present photoluminescence (PL) that can be tuned according with the particle size. Because the quantum dots in SRO present a relatively large size distribution, it is difficult to tune the properties in a directed way. An option to constrain the size of the Si-nCs is to deposit SRO in multilayer structures (MLs) [5].

There are several reports about the PL of SRO, but their study is usually limited to SRO with Si-nCs smaller than 5 nm. For example, PL due to quantum confinement effects in Si-nCs has been observed in Si-implanted SiO_2 films where the PL peak blue-shifted with oxidation time [6]; the largest particles in these films were about 5 nm. The blue-shift has also been reported in sputtered SRO films when varying the Si-nCs sizes from 5 to 2.7 nm [7, 8]. In

1875-3892 © 2012 Published by Elsevier B.V. Selection and/or peer review under responsibility of Chinese Vacuum Society (CVS).
doi:10.1016/j.phpro.2012.03.522

the same way an evident blue shift in the PL could be observed in evaporated MLs containing Si-nCs when the size of the nCs decreases from 3.2 nm to 2.8 nm [5]. SRO films prepared by LPCVD (low pressure chemical vapor deposition) present intense PL when they have a Si excess (excess compared with SiO_2) lower than 8 at% (Ro = 20 – 30), and a weak emission for excess larger than 12 at% (Ro < 10) [9, 10]. One can observe an insignificant blue shift in the PL when going from SRO Ro = 20 to Ro = 30 with particle sizes of around 2.75 nm and no observed particles respectively, but no shift could be observed when decreasing the Ro to 10 (Si-nCs sizes of around 4.2 nm) [9]. These observations may be evidence that the PL in this kind of films is dominated by defects. All results suggest that the PL emission of SRO strongly depends on the size of the Si-nCs embedded in the oxide matrix, independently if it is due to quantum confinement effects or to defects.

In the present work the PL of MLs containing SRO with high silicon content prepared by LPCVD is reported. It is worthy to mention that ML structures of SRO prepared by LPCVD have been previously reported just by our group [11]. The as-deposited MLs contain Si-nCs with average size of 13 nm and do not present PL. The present report deals with the oxidation of these MLs to activate their PL. An emission mechanism of these structures is proposed. Transmission electron microscopy (TEM) and ellipsometry were used to study the structural and compositional properties of the MLs.

2. Experimental details

ML structures composed of stacks of SRO with Ro = 1 (SRO1) and SRO with Ro = 50 (SRO50) were deposited on p-type Si (100) wafers with 30–50 Ωcm resistivity. The deposition was done by LPCVD at 725 °C, using SiH_4 and N_2O as the precursor gases. The MLs are composed of 6 layers of 12 nm of SRO50 alternated with 5 layers of 22 nm of SRO1. The ratio of the precursor gases was varied manually during the deposition to produce the different layers. After the deposition the samples were annealed in N_2 at 1100 °C for 3 hr to segregate Si excess and produce Si-nCs embedded in an oxide matrix. Finally, to vary the size of the Si-nCs, the MLs were oxidized at 800 °C for 30 min in dry oxygen, followed by additional 30 min of oxidation at 800, 900, 1000 or 1100 °C.

The microstructure of the MLs was studied with TEM (Tecnai F30, 300 kV). A Null ellipsometer Gaertner L117, which operates with a 632.8 nm laser at a fix 70° angle of incidence, was used to obtain the refractive index of the samples. The PL emission spectra were obtained with a spectrofluorometer Jobin Yvon Fluoromax-3 at room temperature; the samples were excited with light of 280 nm (4.42 eV), and a long-pass filter of 400 nm (3.1 eV) in the detector was used.

3. Structural characterization

Analyzing several TEM micrographs of the MLs it was possible to do a statistical study of the sizes of the Si-nCs. The size of the Si-nCs decreases upon oxidation temperature. This effect can be clearly observed when comparing the size distributions of the MLs oxidized at 800 (Fig. 1) and 1100 °C (Fig. 2). The sizes of the nCs of the sample oxidized at 800 °C remain close to the sizes in the sample without oxidation. The sizes of the nCs in the sample oxidized at 800 °C can be separated into two ranges: one between ~12 and 20 nm, and the other between 6 and ~12 nm (see Fig. 1). The first range corresponds to the Si-nCs being confined by the thickness of the layers of SRO1 (22 nm), and the second range corresponds to Si-nCs occupying the voids between the larger crystals. In contrast, the sample oxidized at 1100°C consists mainly of nCs smaller than 14 nm, but with some larger crystals still remaining (Fig. 2). An explanation for this distribution could be that the Si-nCs close to the surface are stronger oxidized than those close to the substrate, where some bigger nCs remain after the oxidation process.

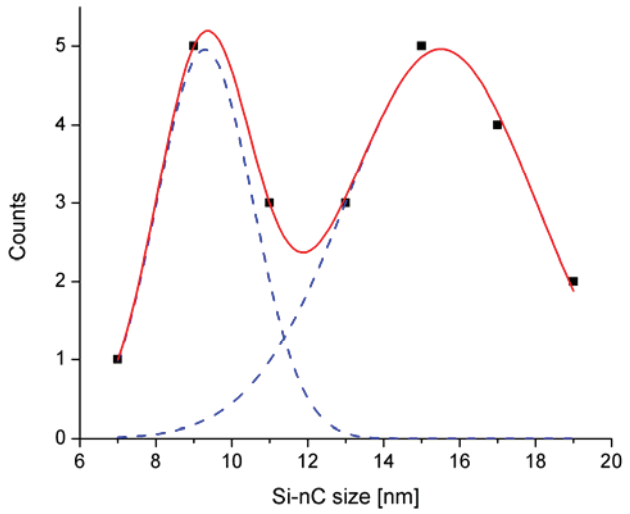

Fig. 1. Size distribution of Si-nCs in the ML oxidized at 800 °C. The dots in the figure represent the measured values. The lines are guides for the eyes.

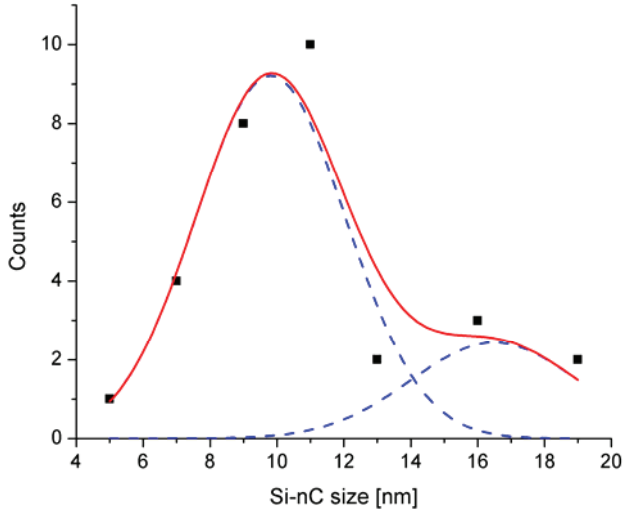

Fig. 2. Size distribution of Si-nCs in the ML oxidized at 1100 °C. The dots in the figure represent the measured values. The lines are guides for the eyes.

To confirm that the amount of Si in the MLs decreases with increasing oxidation temperature, the refraction index of the samples was measured. From the obtained values it was possible to calculate approximately the volume fraction of Si-nCs in the samples using the Bruggeman theory for an effective medium [12]. According to this theory the MLs can be seen as an effective medium with effective refraction index, since the sizes of the Si-nCs and the silicon oxide zones are much smaller than the wavelength of the laser light of the ellipsometer (632.8 nm). The effective refraction index of the studied materials (n_{eff}) is related to the refraction index of each phase (n_{Si} and n_{ox}) as well as to their volume fractions (V_{Si} and V_{ox}). The Bruggeman equation for the two-component system is:

$$V_{Si}\frac{n_{Si}-n_{eff}}{n_{Si}+2n_{eff}}=-V_{ox}\frac{n_{ox}-n_{eff}}{n_{ox}+2n_{eff}} \quad (1)$$

where

$$V_{Si}+V_{ox}=1 \quad (2)$$

The volume fractions of Si-nCs in the different MLs are plotted in Fig. 3. For the calculation the values $n_{ox} = 1.46$ and $n_{Si} = 3.85$ were used. From the plot it can be inferred that the amount of Si transformed into silicon oxides increases when increasing the oxidation temperature.

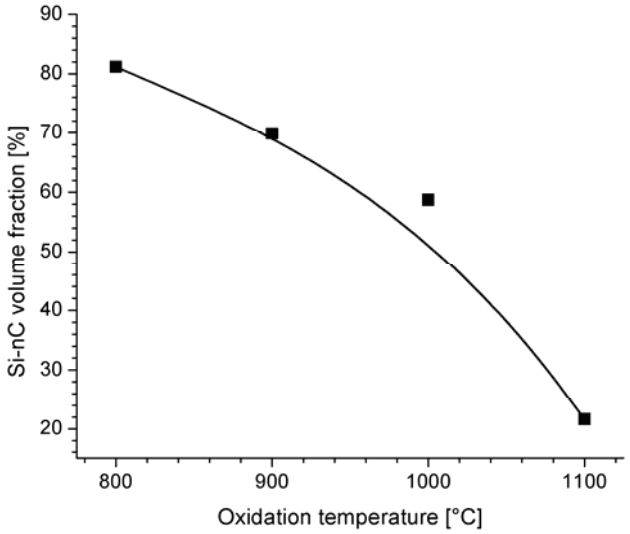

Fig. 3. Plot of the volume fraction of Si-nCs in the MLs oxidized at different temperatures. The dots represent the calculated values, and the solid line is a guide for the eye.

4. Photoluminescence

The PL spectra of the MLs oxidized at 1000 and 1100 °C are shown in Fig. 4 and Fig. 5 respectively. The rest of the samples do not exhibit any detectable PL signal. SRO50 do not exhibit any PL signal. On the other hand, the PL of the luminescent samples cannot be due to direct band-to-band transitions allowed by quantum confinement effects in the nanometric layers of SRO1. If the PL would originate from direct band transitions in the Si-nCs, a blue shift should occur in the PL spectrum of the ML oxidized at 1100 °C compared with that of the ML oxidized at 1000 °C, since the sizes of the Si-nCs in this last sample are bigger. Nevertheless there is not any shift. A deconvolution of the PL peaks was performed in order to give possible explanations to the PL. In both cases the PL spectra can be deconvoluted in two asymmetric peaks centred at around 1.53 (band A) and 1.73 eV (band B), as shown in Fig. 4 and Fig. 5.

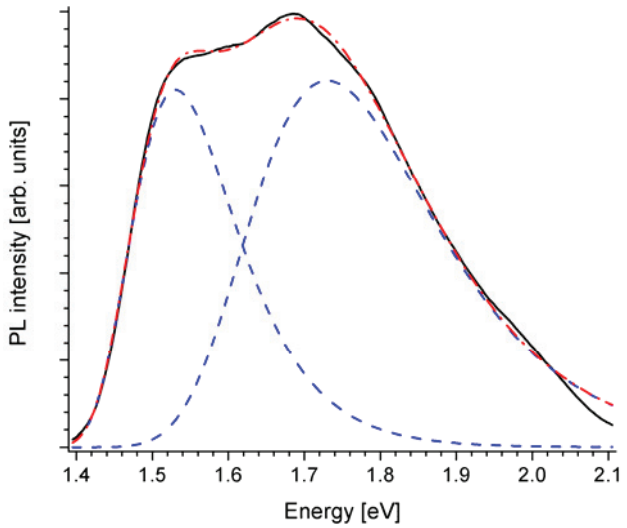

Fig. 4. PL spectrum of the ML oxidized at 1000 °C. It is deconvoluted in asymmetric peaks located approximately at 1.53 and 1.73 eV.

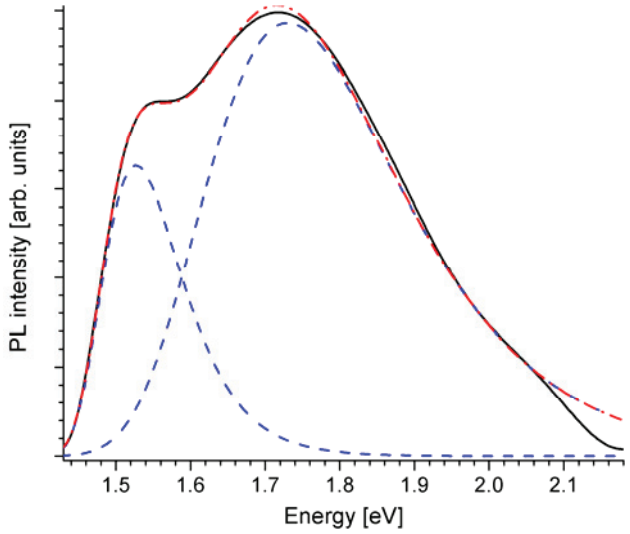

Fig. 5. PL spectrum of the ML oxidized at 1100 °C. It is deconvoluted in asymmetric peaks located approximately at 1.53 and 1.73 eV.

The PL band B has been also observed in SRO with low Si content. For example, the PL of SRO with Ro = 30 prepared by LPCVD presents a maximum at 1.76 eV [10]. This material has a Si excess of around 6 at% [13]. This Si excess does not allow the formation of Si-nCs, but Si sub-oxides [14]. According to this finding, the PL band B from the MLs should be caused by defects in the sub-oxide matrix of the SRO1 layers. Actually there has been reported just an insignificant blue shift in the PL when going from SRO Ro = 20 to Ro = 30 [9], giving evidence of the defect-related PL. Some groups have attributed the PL with energy higher than around 1.7 eV to defects in the oxide matrix [15], especially to non-bonding oxygen hole centres [16]. In the present case the sub-oxides may have reached a configuration close to that in SRO with Ro = 30 upon oxidation, enabling the PL band B. The asymmetric

shape of the band has been also observed in previous reports [17]. In the present MLs the asymmetry of band B remains unaltered when the oxidation temperature is increased.

The position of the peak A also does not change when reducing the size of the Si-nCs, and therefore this peak is not due to direct band transitions in the nCs. This PL peak should then originate from the interfaces between the Si-nCs and the sub-oxide matrix, which is a defect-rich region [18]. The area of band A represents 36.5 % of the PL in the sample oxidized at 1000 °C, and it is reduced to 21.7 % in the sample oxidized at 1100 °C. An explanation for the smaller area of peak A in the sample oxidized at 1100 °C is that part of the Si-nCs are fully oxidized, reducing the intensity of the interface-related PL. In fact the electron diffraction patterns of the two samples (Fig. 6) show that the density of Si-nCs is reduced upon oxidation. The reduction of the density of Si-nC affects also the asymmetry of A. The asymmetry of the band (a = RWHM/LWHM, where RWHM is the right width at half maximum, and LWHM is the left width at half maximum) is 1.42 and 1.6 in MLs oxidized at 1000 and 1100 °C respectively.

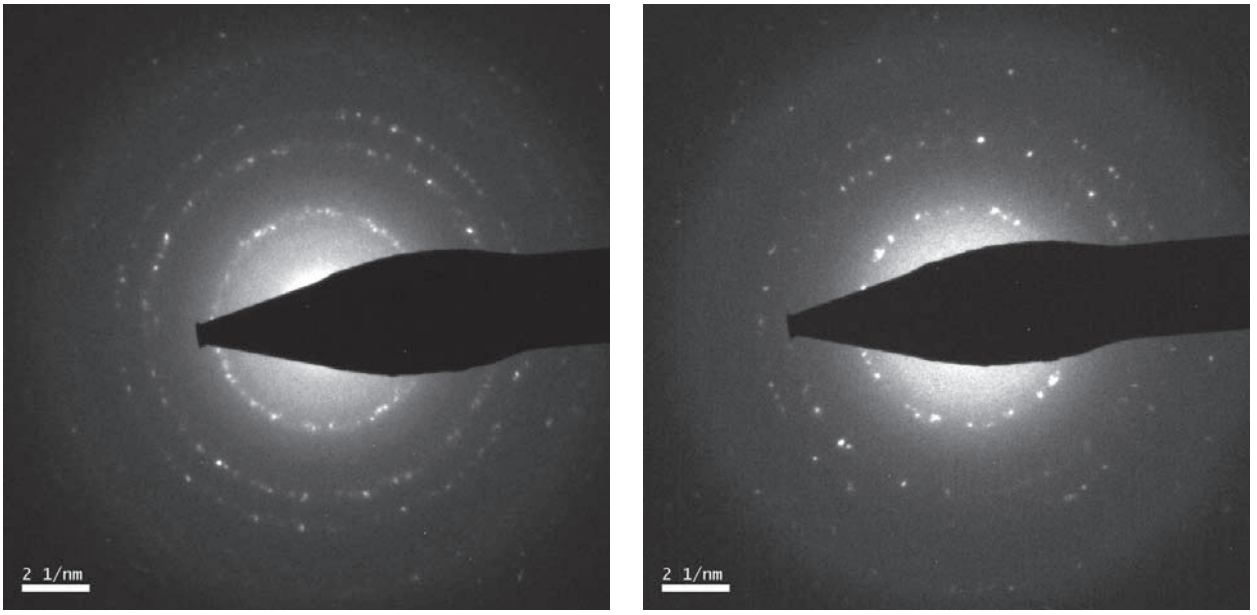

Fig. 6. Electron diffraction patterns of the MLs: left) oxidized at 1000 °C, right) oxidized at 1100 °C. The patterns fit with the metrics for Si.

The MLs oxidized at lower temperatures (800 and 900 °C) do not present PL properties. It is highly likely that the nCs in these samples are not small enough for this emission process. Recently, it has been reported that the PL related to the interface depends strongly on the nC size because quantum confinement effects in the nCs are necessary [19]. Due to the quantum confinement the band gap of the Si-nCs increases when their size decreases, and the breakdown of momentum conservation makes the $\Gamma \rightarrow L$ and $\Gamma \rightarrow X$ transitions pseudo-direct. The defect states are Γ-like and electrons excited from the Si valence band relax to the conduction band edge, from which they tunnel (resonantly) to the defect states and recombine radiatively [20].

5. Conclusion

ML structures containing SRO with high Si content were prepared and PL was activated in them by oxidation. Only the MLs oxidized at higher temperatures present PL. These samples contain the smallest Si-nCs. It was evidenced that the PL is generated by defects in the oxide matrix and by defects located at the interfaces between nanocrystals. The first emission mechanism is independent of the existence of nanocrystals as is the case of SRO

with low Si content. On the other hand, the interface-related PL depends on the size of the Si-nCs. When the Si-nCs have a size at which the band gap of Si is pseudo-direct (a quantum confinement effect), the excited carriers can tunnel to the interfacial defects, where the radiative recombination takes place.

Aknowledgement

The authors appreciate the support of CONACyT and DAAD. They also thank Pablo Alarcón from INAOE for his technical help for the oxidation of the samples.

References

[1] D. Dong, E.A. Irene, D.R. Young, J. Electrochem. Soc.: Solid State Sci. Tech. 125/5 (1978) 819.
[2] E. Talbot, R. Lardé, F. Gourbilleau, C. Dufour, P. Pareige, epl 87 (2009) 26004.
[3] B. Fazio, M. Vulpio, C. Gerardi, Y. Liao, I. Crupi, S. Lombardo, S. Trusso, F. Neri, J. Electrochem. Soc. 149/7 (2002) G376.
[4] Y. Kanemitsu, J. Lumin. 100 (2002) 209.
[5] M. Zacharias, J. Heitmann, R. Scholz, U. Kahler, M. Schmidt, J. Bläsing, Appl. Phys. Lett. 80/4 (2002) 661.
[6] M.L. Brongersma, A. Polman, K.S. Min, E. Boer, T. Tambo, H.A. Atwater, Appl. Phys. Lett. 72/20 (1998) 2577.
[7] Y. Kanzawa, T. Kageyama, S. Takeoka, M. Fujii, S. Hayashi, K. Yamamoto, Solid State Comm. 102/7 (1997) 533.
[8] L. Khomenkova, N. Korsunska, T. Torchynska, V. Yukhimchuk, B. Jumayev, A. Many, Y. Goldstein, E. Savir, J. Jedrzejewski, J. Phys.: Condens. Matter 14 (2002) 13217.
[9] A. Morales-Sánchez, J. Barreto, C. Domínguez-Horna, M. Aceves-Mijares, J.A. Luna-López, Sensors and Actuators A 142 (2008) 12.
[10] R. López-Estopier, M. Aceves-Mijares, C. Falcony, 3rd International Conference on Electrical and Electronics Engineering, IEEE, Mexico City, 2006, p. 1.
[11] E. Quiroga, W. Bensch, Z. Yu, M. Aceves, R.A. De Souza, M. Martin, V. Zaporojtchenko, F. Faupel, Phys. Stat. Sol. A 206/2 (2009) 263.
[12] M. Khardani, M. Bouaïcha, B. Bessaïs, Phys. Stat. Sol. C 4/6 (2007) 1986.
[13] A. Morales, J. Barreto, C. Domínguez, M. Riera, M. Aceves, J. Carrillo, Physica E 38 (2007) 54.
[14] D.J. DiMaria, J.R. Kirtley, E.J. Pakulis, D.W. Dong, T.S. Kuan, F.L. Pesavento, N. Theis, J.A. Cutro, S.D. Brorson, J. Appl. Phys. 56/2 (1984) 401.
[15] M.L. Brongersma, A. Polman, K.S. Min, H.A. Atwater, J. Appl. Phys. 86/2 (1999) 759.
[16] K. Chen, Z. Ma, X. Huang, J. Xu, W. Li, Y. Sui, J. Mei, D. Zhu, J. Non-Cryst. Solids 338-340 (2004) 448.
[17] R. Kiebach, J.A. Luna-López, G.O. Dias, M. Aceves-Mijares, J.W. Swart, J. Mex. Chem. Soc. 52/3 (2008) 212.
[18] F. Djurabekova, M. Backman, K. Nordlund, Nucl. Instrum. Methods Phys. Res. B 266 (2008) 2683.
[19] S. Godefroo, M. Hayne, M. Jivanescu, A. Stesmans, M. Zacharias, O.I. Lebedev, G. Van Tendeloo, V.V. Moshchalkov, Nature Nanotechnology 3 (2008) 174.
[20] B. Averboukh, R. Huber, K.W. Cheah, Y.R. Shen, G.G. Qin, Z.C. Ma, W.H. Zong, J. Appl. Phys. 92/7 (2002) 3564.